Attenuation and Power-Handling Capability of T-Septum Waveguides

YANG ZHANG AND WILLIAM T. JOINES, MEMBER, IEEE

Abstract — **In this paper, the attenuation characteristics and power-handling capabilities of single T-septum waveguides are presented. The analysis is based upon numerical solutions employing the Ritz–Galerkin technique [1]. The analysis was verified by applying it to the known results obtained for the ridged waveguide, which is treated as a special case of the T-septum guide. A good agreement has been achieved compared with the results from Hopfer [2]. It is found that the single T-septum guide can handle less power, but has lower attenuation than the single-ridged guide with identical gap parameters. Equations and charts are presented to facilitate the design of T-septum waveguides.**

I. Introduction

RECTANGULAR waveguides with T-septa inside have been proposed by Mazumder and Saha [3]. Some properties of these waveguides, such as the cutoff wavelength, bandwidth characteristics, and impedance, have been obtained by Zhang and Joines [1] and by Mazumder and Saha [3]. It is shown that the T-septum waveguides have lower cutoff frequencies and broader bandwidths than those of the conventional ridged guides with the same geometries.

In this paper, the analysis based upon the Ritz–Galerkin technique, which is presented in [1], has been extended to obtain the attenuation characteristics and the power-handling capabilities of the single T-septum waveguide (STSG). These properties are compared with those of the single-ridged guide (SRG) with the same gap parameters. Equations and curves are given to facilitate the design of such waveguides. The verification of the theoretical results was carried out by applying the solution to the single-ridged waveguide, treated as a special case of the single T-septum waveguide. A good agreement with the ridged-waveguide results presented by Hopfer [2] was achieved. The derivation presented herein, in combination with the information presented in [1], will give a complete description of the T-septum guide characteristics. With these results, one is able to design any waveguide of this form.

II. T-Septum Guide Attenuation

The geometry of the T-septum waveguide is illustrated in Fig. 1. The analysis of the doubly symmetrical T-septum guide may be analyzed in the same way as the single T-septum guide. The formulation of the problem is to solve an integral eigenvalue problem. The homogeneous equations are solved numerically by the application of the Ritz–Galerkin method to yield a generalized matrix eigenvalue problem. Since the details of formulating the problem can be found in [1], the analysis in this paper directly uses the resultant equations in [1].

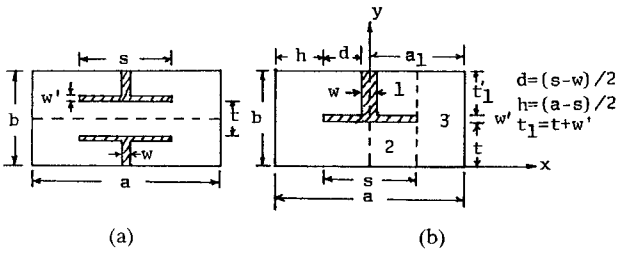

Fig. 1. Geometry of (a) double T-septum guide and (b) single T-septum guide.

The attenuation constant α of the T-septum guide is defined by

$$\alpha = \frac{P_L}{2P} \tag{1}$$

where

$$P = \frac{1}{Z_h}[I_1 + I_2 + I_3] \tag{2}$$

is the propagating power carried by the guide and

$$I_1 = \sum_{n=0}^{\infty} \frac{1}{4}\eta_{1n}^2 \left[(n\pi)^2 \frac{d}{t_1'} \left(1 + \frac{\sin 2k_{x1n}d}{2k_{x1n}d} \right) + 2\epsilon_n k_{x1n}^2 t_1' d \left(1 - \frac{\sin 2k_{x1n}d}{2k_{x1n}d} \right) \right] \tag{3a}$$

$$I_2 = \sum_{m=0}^{\infty} \frac{1}{8}\eta_{2m}^2 \left[(m\pi)^2 \frac{s}{t} \left(1 - \frac{\sin k_{x2m}s}{k_{x2m}s} \right) + 2\epsilon_m k_{x2m}^2 ts \left(1 + \frac{\sin k_{x2m}s}{k_{x2m}s} \right) \right] \tag{3b}$$

$$I_3 = \sum_{p=0}^{\infty} \frac{1}{4}\eta_3^2 \left[(p\pi)^2 \frac{h}{b} \left(1 + \frac{\sin 2k_{x3p}h}{2k_{x3p}h} \right) + 2\epsilon_p k_{x3p}^2 bh \left(1 - \frac{\sin 2k_{x3p}h}{2k_{x3p}h} \right) \right]. \tag{3c}$$

Manuscript received February 23, 1987; revised April 18, 1987.

The authors are with the Department of Electrical Engineering, Duke University, Durham, NC 27706.

IEEE Log Number 8715666.

The terms in (3) are defined as follows:

$$\eta_{1n} = \frac{-A_n}{k_{x1n}\sin k_{x1n}d} \tag{4a}$$

$$\eta_{2m} = \frac{B_m}{k_{x2m}\cos k_{x2m}s/2} \tag{4b}$$

$$\eta_{3p} = \frac{1}{\epsilon_p b k_{x3p}\sin k_{x3p}h}\sum_{J=0}^{J}\left(A_J P_{1JP} B_J P_{2JP}\right) \tag{4c}$$

where $\epsilon_0 = 1$ and $\epsilon_p = 0.5$ for $p \neq 0$, and

$$k_{x1n} = \begin{cases} \sqrt{k_c^2 - \left(\dfrac{n\pi}{t_1'}\right)^2} & k_c \geq \dfrac{n\pi}{t_1'} \quad (5a) \\ -j\sqrt{\left(\dfrac{n\pi}{t_1'}\right)^2 - k_c^2} & k_c \leq \dfrac{n\pi}{t_1'}. \quad (5b) \end{cases}$$

The quantities k_{x2m} and k_{x3p} are defined similarly, and

$$P_{1JP} = \int_{t_1}^{b}\cos\frac{j\pi}{t_1'}(y - t_1')\cos\frac{p\pi}{b}(y-b)\,dy \tag{6}$$

$$P_{2JP} = \int_{0}^{t}\cos\frac{j\pi}{t}(y - t)\cos\frac{p\pi}{b}(y-b)\,dy \tag{7}$$

$$[A] = [A_1, A_2, \cdots, A_J]^T \tag{8}$$

$$[B] = [B_1, B_2, \cdots, B_J]^T. \tag{9}$$

The vector $[A|B]^T$ is the eigenvector for a particular eigenvalue k_c of the following eigensystem:

$$[H_A(k_c)|H_B(k_c)]\begin{bmatrix} A \\ B \end{bmatrix} = [0]. \tag{10}$$

The eigenvalue k_c is the solution of the nonlinear equation

$$\det|H_A(k_c)|H_B(k_c)| = 0. \tag{11}$$

The matrix elements $H_A(k_c)$ and $H_B(k_c)$ are given in [1].

The power loss per unit length is [4]

$$P_L = \frac{1}{2}R_m Y_h^2 \oint_c \left[|\boldsymbol{n}\times\nabla_t g(x,y)|^2 + \frac{k_c^4}{k^2 - k_c^2}g^2(x,y)\right]dl \tag{12}$$

where $R_m = \sqrt{\omega\mu/2\sigma}$ is the skin-effect surface resistance of a metal with permeability μ. $Z_h = 1/Y_h$ is the wave impedance of the guide; and $k = \omega\sqrt{\mu\epsilon}$ is the wavenumber; $\boldsymbol{n}$ is the unit vector normal to the integral contour; and $g(x, y)$ is the Hertzian potential derived in [1] as

in region 1:

$$g_1(x,y) = \sum_{n=0}^{\infty}\eta_{1n}\cos k_{x1n}\left(x - \frac{w}{2}\right)\cos\frac{n\pi}{t_1'}(y - t_1) \tag{13}$$

in region 2:

$$g_2(x,y) = \sum_{m=0}^{\infty}\eta_{2m}\sin k_{x2m}x\cos\frac{m\pi}{t}(y-t) \tag{14}$$

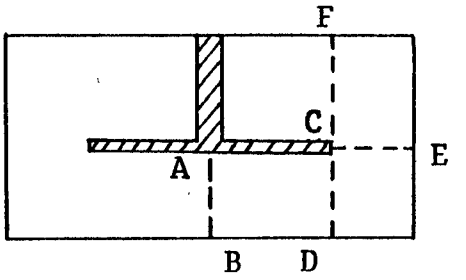

Fig. 2. The single T-septum guide. The maximum electric field is assumed to be on line AB, CD, CE, or CF.

in region 3:

$$g_3(x,y) = \sum_{p=0}^{\infty}\eta_{3p}\cos k_{x3p}(x - a_1)\cos\frac{p\pi}{b}(y-b). \tag{15}$$

The line integration of (12) is performed along all the walls and the T-septum of the guide.

III. Power-Handling Capability

The electric fields inside the T-septum waveguide are [1]

in region 1:

$$\boldsymbol{e}_1(x,y) = \sum_{n=0}^{\infty}\eta_{1n}\left[\frac{n\pi}{t_1'}\cos k_{x1n}\left(x - \frac{w}{2}\right)\sin\frac{n\pi}{t_1'}(y - t_1)\boldsymbol{a}_x - k_{x1n}\sin k_{x1n}\left(x - \frac{w}{2}\right)\cos\frac{n\pi}{t_1'}(y - t_1)\boldsymbol{a}_y\right] \tag{16}$$

in region 2:

$$\boldsymbol{e}_2(x,y) = \sum_{m=0}^{\infty}\eta_{2m}\left[\frac{m\pi}{t}\sin k_{x2m}x\sin\frac{m\pi}{t}(y-t)\boldsymbol{a}_x + k_{x2m}\cos k_{x2m}x\cos\frac{m\pi}{t}(y-t)\boldsymbol{a}_y\right] \tag{17}$$

in region 3:

$$\boldsymbol{e}_3(x,y) = \sum_{p=0}^{\infty}\eta_{3p}\left[\frac{p\pi}{b}\cos k_{x3p}(x - a_1)\sin\frac{p\pi}{b}(y-b)\boldsymbol{a}_x - k_{x3p}\sin k_{x3p}(x - a_1)\cos\frac{p\pi}{b}(y-b)\boldsymbol{a}_y\right]. \tag{18}$$

The power-handling capability may be determined by setting the maximum electric field inside the guide equal to the breakdown intensity of the dielectric filling the guide, and calculating the propagating power P_m accordingly. Thus, P_m is seen to represent the maximum power which could possibly be handled by the T-septum guide. In this paper, air-filled waveguides are considered, and a breakdown electric field of 30 kV/cm is assumed.

The single T-septum guide is shown in Fig. 2. We assume that the maximum electric field might occur along lines AB, CD, CE, or CF. Thus, we calculate the magnitudes of the electric fields along lines AB, CD, CE, and CF, and choose the maximum among these values as the maximum electric field inside the guide. We then calculate the propagating power accordingly. The propagating power thus obtained would be the maximum power that the waveguide can handle. One should consider a safety factor when applying the curves presented below.

IV. Numerical Results

In order to present T-septum guide attenuation data in a general fashion, it is convenient to compare the attenuation of the T-septum guide to that of a rectangular guide of identical cutoff frequency. We thus define a normalized attenuation α_n as the ratio of the T-septum guide attenuation to the rectangular guide attenuation of identical cutoff and evaluate this ratio at a frequency $f=\sqrt{3}f_c$. The maximum propagating power P_m is calculated at $f=\infty$ and normalized to λ_c^2; thus, only relative dimensions of the guide are required in the calculations. The maximum propagating power at any other frequency is obtained by multiplying P_m/λ_c^2 by $[1-(f_c/f)^2]^{1/2}$.

To check the correctness of the analysis, the single-ridged waveguides of various geometries were analyzed. In this case, the T-septum guide is made to approach a ridged guide by setting $w=s$; i.e., the septum degenerates into a solid ridge. A comparison of the present results with those from Hopfer [2] is illustrated in Table I. The data show that the present results agree quite well with the known results for the single-ridged guide, the range of difference being 0.3–10 percent. In some limiting cases where t/b is very small for the attenuation, or very large for the maximum power, a difference of about 23–28 percent was obtained. This might be due to the approximations used by Hopfer in his derivation of parameters.

In Figs. 3 and 4, the relative attenuation for aspect ratios of 0.45 and 0.25 are plotted as a function of s/a, with t/b as a parameter. The chosen values of septum thickness ratios are $w'/b=0.05$ and $w/a=0.10$. In the calculations of the attenuation data, it is assumed that the aspect ratio b/a of the rectangular guide is the same as that of the T-septum guide. In order to evaluate the actual attenuation of the T-septum guide at $f=\sqrt{3}f_c$, α_n must be multiplied by the rectangular guide attenuation at this frequency. This latter quantity may be found in many reference works, for example [5]. Superposed as dashed lines in Fig. 3 are the attenuation data for single-ridged guides [2] with identical t/b and s/a, subject to the error in reproducing the curves. No ridged-guide data are readily available for $b/a=0.25$. Therefore, the comparison is limited to $b/a=0.45$. Note that the relative attenuation of the T-septum guide increases monotonically with s/a for fixed t/b and is less than that of SRG for s/a less than 0.60. For s/a greater than about 0.60, SRG has less attenuation. If s/a is fixed, the attenuation of the T-septum guide decreases as t/b increases.

Figs. 5 and 6 show the power-handling capabilities of STSG of two aspect ratios, 0.45 and 0.25, respectively. The dashed lines in Fig. 5 are the corresponding properties of SRG of the same aspect ratio. It is found that the maximum power that a STSG can possibly handle is almost a constant for s/a less than 0.8 when t/b is fixed, and is always less than that for a SRG. For s/a greater than 0.8, i.e., the septum is very close to the side walls, P_m/λ_c^2 drops drastically. In this case, the breakdown occurs between the septum and the side walls, rather than at the center of the septum. No SRG data are available for s/a greater than 0.7, but it seems reasonable to conclude that the results would be similar. Also note that if s/a is fixed, P_m/λ_c^2 increases as t/b increases.

TABLE I
Confirmation of the Present Analysis

t/b	Hopfer		Present	
	α_n	P_m/λ_c^2	α_n	P_m/λ_c^2
0.10	13.4	0.61	9.582	0.608
0.15	7.6	1.30	6.050	1.387
0.20	5.3	2.30	4.428	2.509
0.25	4.0	3.90	3.620	4.027
0.30	3.1	5.90	3.038	5.975
0.35	2.7	8.10	2.628	8.377
0.40	2.3	9.10	2.318	11.257

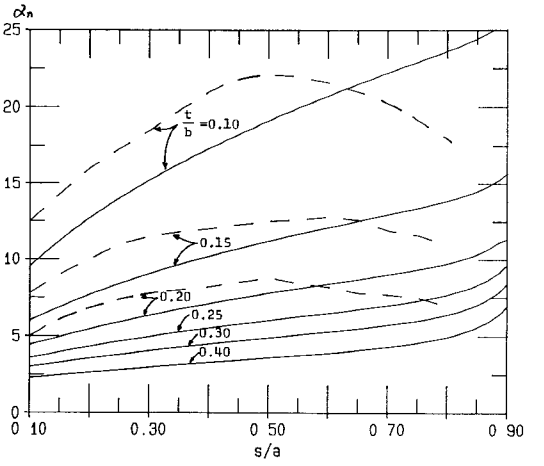

Fig. 3. Variation of normalized attenuation with gap width ratio (s/a). Solid lines: single T-septum guide; dashed lines: single ridged guide of the same geometry with solid ridge ($w=s$). Here $b/a=0.45$, $w/a=0.10$, $w'/b=0.05$, and $f=\sqrt{3}f_c$.

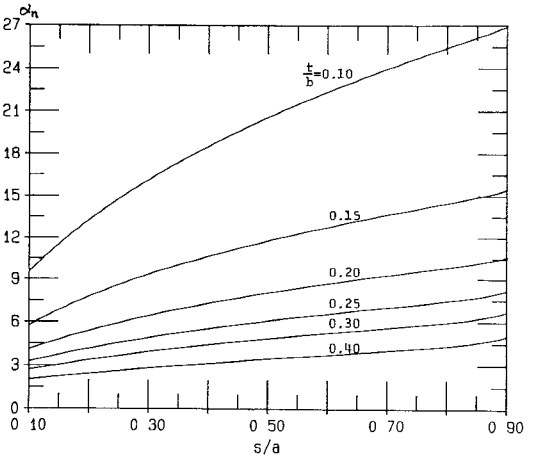

Fig. 4. Variation of normalized attenuation with gap width ratio (s/a). $b/a=0.25$, $w/a=0.10$, $w'/b=0.05$, and $f=\sqrt{3}f_c$.

The following numerical example will illustrate an application of our results. If a particular single T-septum guide has $b/a=0.45$, $w/a=0.10$, $w'/b=0.05$, $t/b=0.30$, and $s/a=0.70$, we find from Figs. 3 and 5 at $f=\sqrt{3}f_c$ that $\alpha_n=7.0$ and $P_m/\lambda_c^2=6.85\text{kW/cm}^2$ or $P_m=164.5a^2$ kW. This means that the attenuation of the guide is seven times greater than that of a rectangular guide of

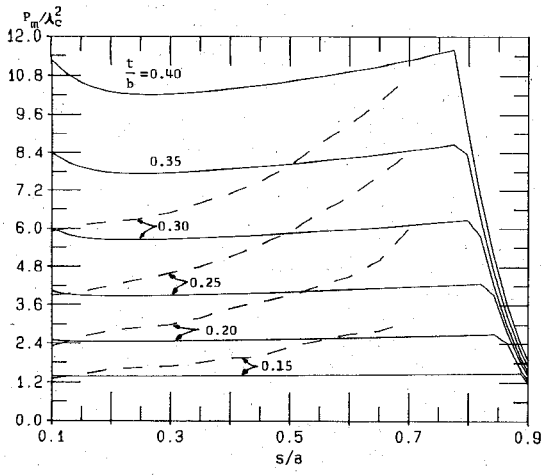

Fig. 5. Power-handling capability P_m/λ_c^2 in kW/cm^2 at $f=\infty$ versus gap width ratio (s/a). Solid lines: single T-septum guide; dashed lines: single ridged guide of the same geometry with solid ridge ($w=s$). $b/a=0.45$, $w/a=0.10$, and $w'/b=0.05$. For any other frequency, multiply the ordinate by $[1-(f_c/f)^2]^{1/2}$.

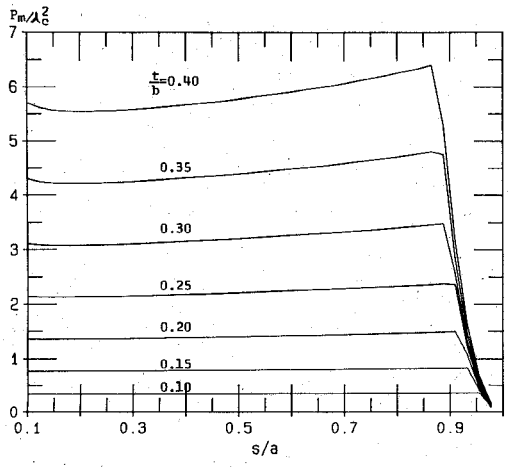

Fig. 6. Power-handling capability P_m/λ_c^2 in kW/cm^2 at $f=\infty$ versus gap width ratio (s/a). $b/a=0.25$, $w/a=0.10$, and $w'/b=0.05$. For any other frequency, multiply the ordinate by $[1-(f_c/f)^2]^{1/2}$.

identical cutoff frequency and aspect ratio, and that the maximum power that the T-septum guide can handle is $164.5a^2$ kW, where a is in cm.

V. Discussion

The T-septum guide properties presented in this paper in combination with those published in [1] and [3] form a complete study of the T-septum guide. It has been shown that such a waveguide, compared with the ridged guide, has much lower cutoff frequency, broader bandwidth, and lower attenuation. The flatness of P_m/λ_c^2 versus s/a when $s/a<0.8$ for fixed t/b will allow us to choose s/a to optimize the cutoff frequency and bandwidth. For $s/a=0.45$, the relative attenuation of the STSG is about 30 percent less than that of the SRG. The maximum power that the STSG can handle is about 25 percent less than that of the SRG of identical dimensions. However, the advantages of increased bandwidth, lower cutoff frequency, and lower attenuation should outweigh the disadvantage of lower power-handling capability.

References

[1] Y. Zhang and W. T. Joines, "Some properties of T-septum waveguides," *IEEE Trans. Microwave Theory Tech.* vol. MTT-35, pp. 769–775, Aug. 1987.

[2] S. Hopfer, "The design of ridged waveguides," *IRE Trans. Microwave Theory Tech.*, vol. MTT-3, pp. 20–29, Oct. 1955.

[3] G. G. Mazumder and P. K. Saha, "Rectangular waveguide with T-shaped septa," *IEEE Trans. Microwave Theory Tech.*, vol. MTT-35, pp. 201–204, Feb. 1987.

[4] R. E. Collin, *Field Theory of Guided Waves*. New York: McGraw-Hill, 1960, ch. 5, p. 183.

[5] N. Marcuvitz, *Waveguide Handbook*. New York: McGraw-Hill, 1951, ch. 2, p. 61.

Yang Zhang was born in Shenyang, China, on December 5, 1957. He received the B.S.E.E. degree with high honors from Chengdu Institute of Radio Engineering, Chengdu, China, in 1982 and the M.S. degree in electrical engineering from Duke University, Durham, NC, in 1984. He is presently with the Department of Electrical Engineering, Duke University, as a Research Assistant, where he is working towards the Ph.D. degree in microwave engineering.

His research interests are in the area of electromagnetic wave interactions with materials, with applications to transmission lines, and antennas, and microwave-induced hyperthermia. Mr. Zhang is a member of Eta Kappa Nu honorary professional society.

William T. Joines (M'61) was born in Granite Fall, NC on November 20, 1931. He received the B.S.E.E. degree with high honors from North Carolina State University, Raleigh, in 1959 and the M.S. and Ph.D. degrees in electrical engineering from Duke University, Durham, NC, in 1961 and 1964, respectively.

From 1959 to 1966, he was a member of the Technical Staff at Bell Laboratories, Winston-Salem, NC, where he was engaged in research and development of microwave components and systems from military applications. He joined the faculty of Duke University in 1966, and is currently a Professor of Electrical Engineering. His research and teaching interests are in the area of electromagnetic wave interactions with materials.